

**BIAXIAL THERMAL CREEP OF V-4Cr-4Ti AT 700°C AND 800°C – R. J. Kurtz and M. L. Hamilton (Pacific Northwest National Laboratory)\***

**OBJECTIVE**

To determine the biaxial thermal creep characteristics of V-4Cr-4Ti over the temperature range 600 to 800°C at realistic stresses for comparison with uniaxial creep tests and irradiation creep experiments.

**SUMMARY**

A study of the thermal creep properties of V-4Cr-4Ti is being performed using pressurized tube specimens. Creep tubes nominally 4.572 mm OD and 0.254 mm wall thickness were pressurized with high-purity helium gas to mid-wall effective stress levels below the uniaxial yield strength at the test temperature of interest. Specimens are being heated to 700 and 800°C in an ultra-high vacuum furnace and held at temperature for specific time intervals. Periodically the specimens are removed to measure the change in OD with a high-precision laser profilometer. Initial results show that creep rates at 800°C are substantially greater than at 700°C.

**PROGRESS AND STATUS**

Introduction

Vanadium-base alloys are attractive candidate materials for fusion first-wall/blanket structural materials, in part, because of their potentially high service temperatures. Information on the time-dependent, high-temperature deformation properties of vanadium and vanadium alloys is limited, and within the existing data base there are uncertainties which may have influenced the results such as the interstitial impurity content of test specimens and vacuum quality. Because of this paucity of data it is a priority for the U.S. Advanced Materials Program to characterize the creep and creep rupture properties of the reference vanadium alloy V-4Cr-4Ti.

To develop a suitable test matrix, the pertinent data on thermal creep of pure vanadium and vanadium alloys was collected and summarized [1-8]. Wheeler, et al. [1] determined the secondary creep rate of pure polycrystalline vanadium over the temperature range from 477 to 1600°C. Their results showed that the activation energy for creep increased linearly from 234 to 507 kJ/mole as the stress decreased from 147 MPa to 2.5 MPa. The activation energy for creep was seen to be larger than that for self-diffusion at any given temperature.

A fifth power dependence of the minimum creep rate on applied stress was found when the ratio of strain rate to diffusivity was less than  $10^9 \text{ cm}^{-2}$ . Above this ratio a stronger stress dependence was observed. Figure 1 presents a graph of the stress dependence of the minimum creep rate for pure vanadium over the temperature range of 600 to 850°C. The 650 and 800°C data in Figure 1 were generated by Shirra [2]. Note the stress exponent is about 11.3 at stresses above 40 MPa but drops to 6.2 at stress levels below 30 MPa.

---

\*Pacific Northwest National Laboratory (PNNL) is operated for the U.S. Department of Energy by Battelle Memorial Institute under contract DE-AC06-76RLO-1830.

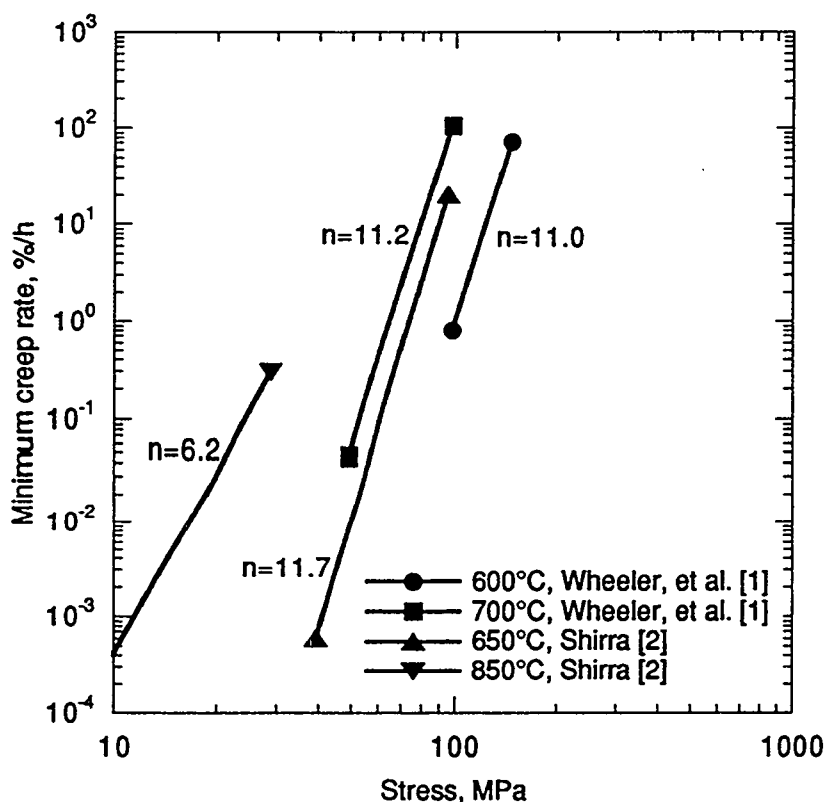


Figure 1 . Stress dependence of the minimum creep rate of pure vanadium.

The stress dependence of the secondary creep rate for V-Ti alloys is similar to that for pure vanadium [3-6]. The available data suggests that for Ti concentrations around 5 w/o, temperatures in the 650 to 700°C range, and stress levels above about 200 MPa the stress exponent is around 11. The stress exponent decreased to values between 2 and 6 for specimens with higher Ti content and tested at higher temperatures and lower stresses. Higher titanium levels have been observed to increase the secondary creep rate.

The creep behavior of V-Cr-Ti alloys tested between 600 and 800°C is plotted in Figure 2 [7,8]. The Ti concentration was about 4 to 5 w/o while the Cr concentration ranged from 4 to 15 w/o. The creep resistance of V-Cr-Ti alloys appears to increase with increasing Cr level, although this observation is not unequivocal. The stress exponent is between 10 and 11 for the bulk of these data. It should be noted that all of the creep data shown in Figure 2 was generated at stress levels greater than 200 MPa. Recently summarized tensile property data for V-4Cr-4Ti [9-11] shows that stresses of this magnitude are very close to the yield strength at temperatures between 300 and 700°C. Furthermore, a preliminary design analysis for V-4Cr-4Ti using the procedures given in the ASME Boiler and Pressure Vessel Code and the ITER Interim Structural Design Criteria indicates that the primary membrane stress limit in the temperature range of 500 to 700°C is about 110 MPa [12]. Thus, the initial test matrix was selected to explore the thermal creep properties of V-4Cr-4Ti at stress levels bounding the conditions that a vanadium first-wall structural material might experience.

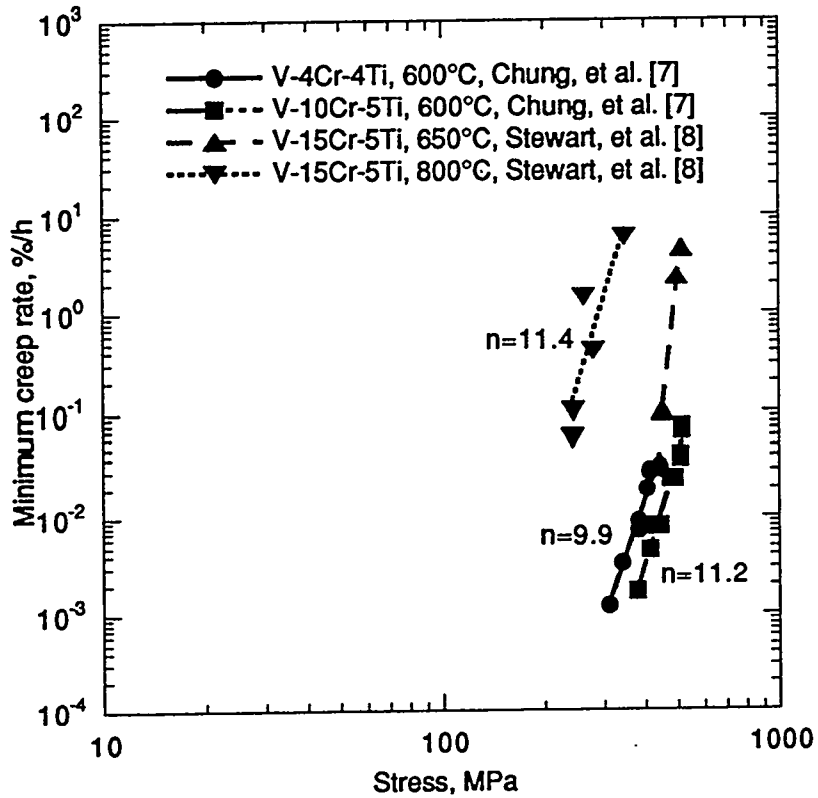


Figure 2. Stress dependence of the minimum creep rate of V-Cr-Ti alloys between 600-800°C.

Table 1 lists the temperatures and mid-wall hoop stress levels planned for the initial series of experiments. Since the ratio of inner radius to wall thickness for our creep tubes is less than 10, it is more appropriate to calculate tube stresses using the expressions for a thick-wall cylinder rather than the approximate thin-wall equations. The mid-wall hoop stresses given in Table 1 were obtained from

$$\sigma_h = \frac{pR_i^2}{R_o^2 - R_i^2} \left[ 1 + \frac{R_o^2}{R_m^2} \right] \quad (1)$$

where  $R_o$  is the outer radius,  $R_i$  is the inner radius,  $p$  is the internal pressure at the test temperature and  $R_m$  is the mid-wall radius. As highlighted in Table 1 by bold italicized entries the first tests will focus on the 700 and 800°C temperatures since these should be completed in the shortest time. It should be noted the stress levels and test temperatures may be revised and updated to reflect early results.

### Experimental Procedure

Sections of V-4Cr-4Ti tubing with a nominal 4.572 mm OD, 0.254 mm wall thickness and ~45% cold work level were obtained from Argonne National Laboratory (ANL) for fabricating

Table 1. Planned matrix for biaxial thermal creep experiments. *Italicized values represent specimens tested during the first campaign.*

Test Temp., °C	Mid-Wall Hoop Stress, MPa					
600	100	150	175	200	225	250
700	<i>75</i>	<i>100</i>	<i>125</i>	<i>150</i>	<i>175</i>	200
800	25	50	<i>75</i>	<i>100</i>	<i>125</i>	<i>150</i>

creep specimens. Figure 3 shows a sketch of the specimen geometry including end-caps. Details of the tubing fabrication have been reported previously [13]. Specimen blanks 25.4 mm long were cut from the tubing and measurements of the ID and OD were performed at two axial locations ( $x/L = 1/3$  and  $2/3$ ) and at  $45^\circ$  azimuthal intervals prior to cleaning. Specimen blanks and end-caps were then prepared for welding by cleaning in accordance with modified ANL Procedure IPS-181-00-00. The modifications to this procedure included a somewhat shorter exposure to the pickling solution (~3 min.) and deletion of the oven drying step. Following cleaning, specimen thickness was measured using a metallurgical microscope at eight equally spaced azimuthal locations around each tube end. Five TEM disks punched from pure titanium foil were inserted into each specimen and end-caps were electron-beam welded to the tubes. Following end-cap welding the specimens were loosely wrapped with titanium foil and annealed in a vacuum ( $\leq 10^{-7}$  torr) at  $1000^\circ\text{C}$  for 1 h. After heat treatment specimen ODs were re-measured using a laser profilometer. The sensitivity of the laser profilometer is  $\pm 5 \times 10^{-4}$  mm which translates to a strain measurement sensitivity of about  $\pm 0.01\%$ . The diameter measurements were made at five axial locations ( $x/l$  of 0.1, 0.3, 0.5, 0.7 and 0.9). Specimens were then filled with 99.999% purity helium gas to the desired pressure and sealed by laser welding. Fill pressures were determined with a computer code that accounted for the thermal expansion of the tubing and compressibility of the helium fill gas at the test temperature of interest. The specimen OD was again measured using the laser profilometer to determine the elastic diametral displacements for each tube. Table 2 summarizes the pre-fill dimensional measurements for each specimen currently under test along with the fill pressures and mid-wall hoop stresses.

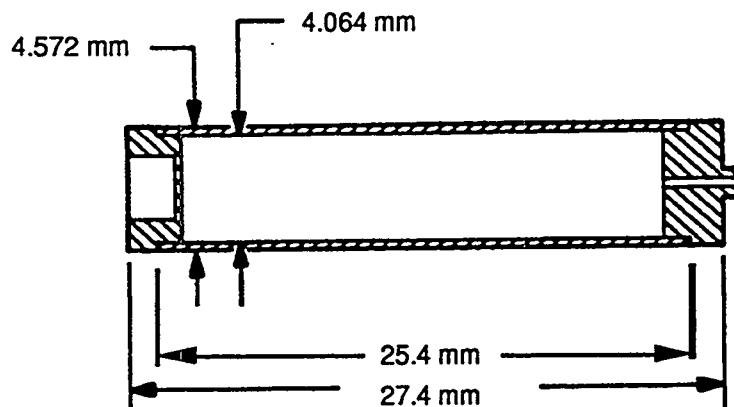


Figure 3. Sketch of creep tube specimen geometry.

Table 2. Unpressurized creep tube dimensions, fill pressures and mid-wall hoop stress levels.

Test Temp., °C	Specimen Code	Specimen OD, mm	Specimen Wall, mm	Fill Press., MPa	Mid-Wall Hoop Stress, MPa
700	AR11	4.5674	0.2601	2.896	72.5
	AR12	4.5662	0.2532	3.909	99.9
	AR13	4.5672	0.2456	4.937	129.6
	AR14	4.5657	0.2499	5.930	151.9
	AR15	4.5659	0.2553	6.964	173.4
800	AR16	4.5684	0.2477	2.654	77.3
	AR17	4.5667	0.2507	3.571	101.2
	AR18	4.5664	0.2461	4.482	128.7
	AR19	4.5667	0.2543	5.419	149.4

Prior to insertion into the vacuum furnace each specimen was loosely wrapped with titanium foil to provide additional protection against oxygen pickup during the experiment. Initially tube diameters were measured weekly until it was apparent that longer intervals could be tolerated. Testing will be conducted for several months to permit measurement of secondary creep rates and in some cases the time to failure. Two tube sections without end-caps were also included with the pressurized specimens at each test temperature to enable periodic assays for oxygen pickup.

### Results

Tube diameters were measured as a function of time using the same equipment, procedures and personnel as before test. Tables 3 and 4 give the time dependence of the specimen diameter and effective mid-wall creep strains for the 700 and 800°C test temperatures, respectively. To preclude end effects only the middle three measurements along the length of the tube were used to compute the average diametral strain. For failed specimens the creep strain is based on the diameter measurement taken nearest to the failure location. Creep strains were calculated from the total measured strain minus the elastic contribution. Conversion from outer diameter strain to mid-wall strain was done using the expression derived by Gilbert and Blackburn [14]. It should be noted the conversion factor is only a constant for very small strain levels. The conversion factor decreases with increasing strain. The Gilbert and Blackburn expressions were evaluated numerically to give values of the conversion factor up to diametral strains of 0.3. The results are plotted in Figure 4. Mid-wall hoop strains were converted to effective strains by

$$\varepsilon_e = \frac{2}{\sqrt{3}} \varepsilon_h \quad (2)$$

where  $\varepsilon_e$  is the effective mid-wall creep strain and  $\varepsilon_h$  is the mid-wall hoop strain. The results in Tables 3 and 4 are plotted in Figures 5 and 6. Effective mid-wall stresses obtained from the Von Mises distortion energy criterion are presented in Figures 5 and 6 rather than the mid-wall hoop stresses. The principal stresses inserted into the Von Mises equation were

the appropriate expressions for stress in a thick-wall, closed end cylinder. The ratio of mid-wall effective stress to mid-wall hoop stress is given by

$$\frac{\sigma_e}{\sigma_h} = \frac{\sqrt{3}R_o^2}{R_o^2 + R_m^2} \quad (3)$$

where  $\sigma_e$  is the effective mid-wall stress and all other variables are the same as above.

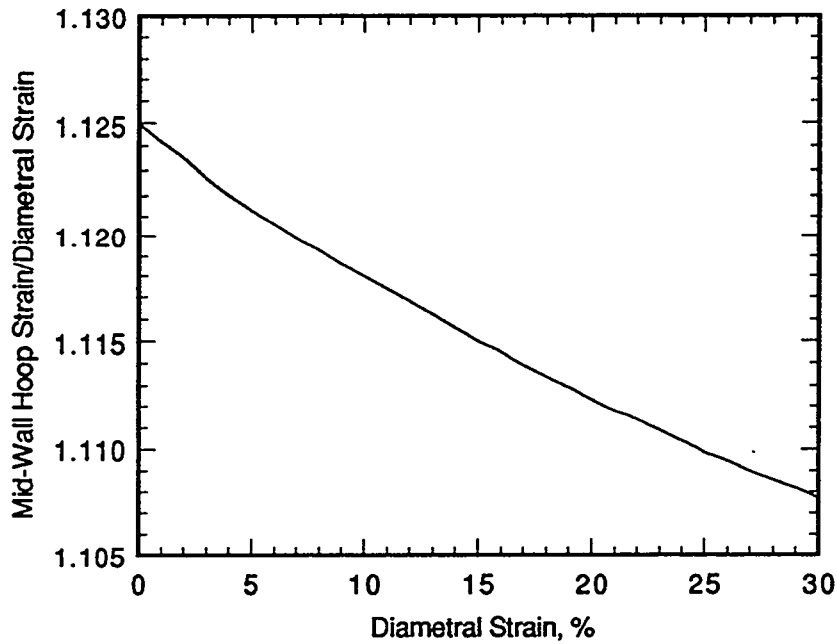


Figure 4. Ratio of mid-wall hoop strain to diametral strain as a function of diametral strain.

Table 3. Time dependence of specimen diameter and effective mid-wall creep strain for 700°C tests.

Time, h	AR11		AR12		AR13		AR14		AR15	
	OD*	$\epsilon_e$ **	OD	$\epsilon_e$	OD	$\epsilon_e$	OD	$\epsilon_e$	OD	$\epsilon_e$
0	4.5682	0.0000	4.5674	0.0000	4.5687	0.0000	4.5672	0.0000	4.5674	0.0000
168	4.5684	0.0072	4.5674	0.0000	4.5690	0.0072	4.5674	0.0072	4.5682	0.0217
242	4.5684	0.0072	4.5674	0.0000	4.5690	0.0072	4.5677	0.0145	4.5687	0.0361
357	4.5684	0.0072	4.5677	0.0072	4.5690	0.0072	4.5682	0.0289	4.5702	0.0795
598	4.5684	0.0072	4.5682	0.0217	4.5692	0.0145	4.5692	0.0578	4.5748	0.2096
1375	4.5684	0.0072	4.5679	0.0145	4.5695	0.0217	4.5715	0.1229	4.5999	0.9246
1523	4.5684	0.0072	4.5674	0.0000	4.5700	0.0361	4.5720	0.1373	4.6124	1.2783

\*Outer diameter in mm.

\*\* $\epsilon_e$  = effective mid-wall strain, %

Table 4. Time dependence of specimen diameter and effective mid-wall creep strain for 800°C tests.

Time, h	AR16		AR17		AR18		AR19	
	OD*	$\epsilon_e$ **	OD	$\epsilon_e$	OD	$\epsilon_e$	OD	$\epsilon_e$
0	4.5695	0.0000	4.5674	0.0000	4.5679	0.0000	4.5677	0.0000
168	4.5705	0.0289	4.5697	0.0650	4.5730	0.1445	4.6942	3.5917
242	4.5707	0.0361	4.5715	0.1156	4.5898	0.6212	5.0874	14.709
412	4.5735	0.1156	4.5959	0.8089	4.7724	5.7999	-	-
488	4.5758	0.1806	4.6213	1.5306	4.9507	10.832	-	-
578	4.5817	0.3466	4.6708	2.9363	5.4242	24.141	-	-
727	4.5989	0.8375	4.7937	6.4173	-	-	-	-
864	4.6228	1.5156	5.0013	12.290	-	-	-	-
1031	4.6622	2.6327	-	-	-	-	-	-
1343	4.7615	5.4454	-	-	-	-	-	-
1491	4.8204	7.1108	-	-	-	-	-	-
1784	4.9525	10.835	-	-	-	-	-	-

\*Outer diameter in mm.

\*\* $\epsilon_e$  = effective mid-wall strain, %

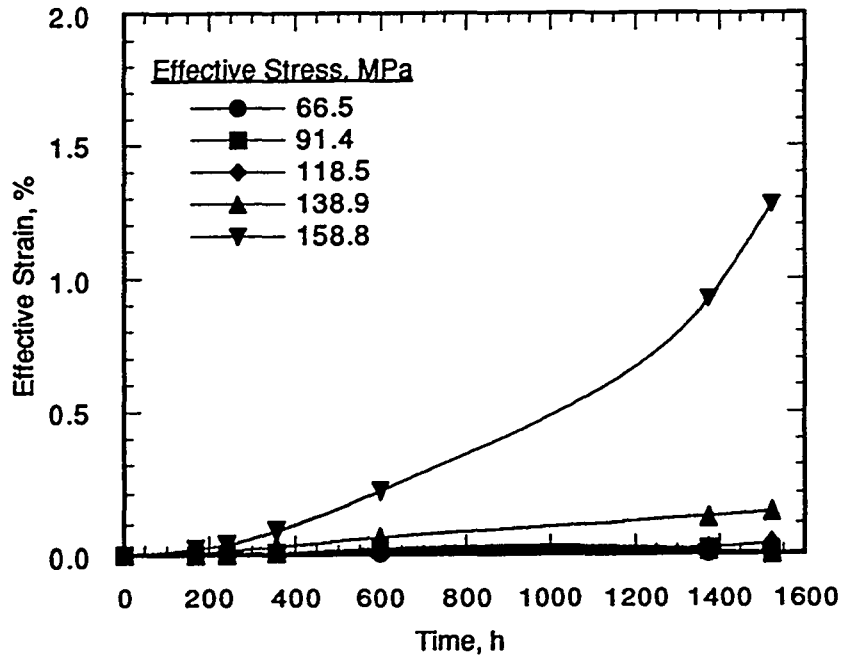


Figure 5. Time dependence of effective mid-wall creep strain at 700°C for unirradiated V-4Cr-4Ti.

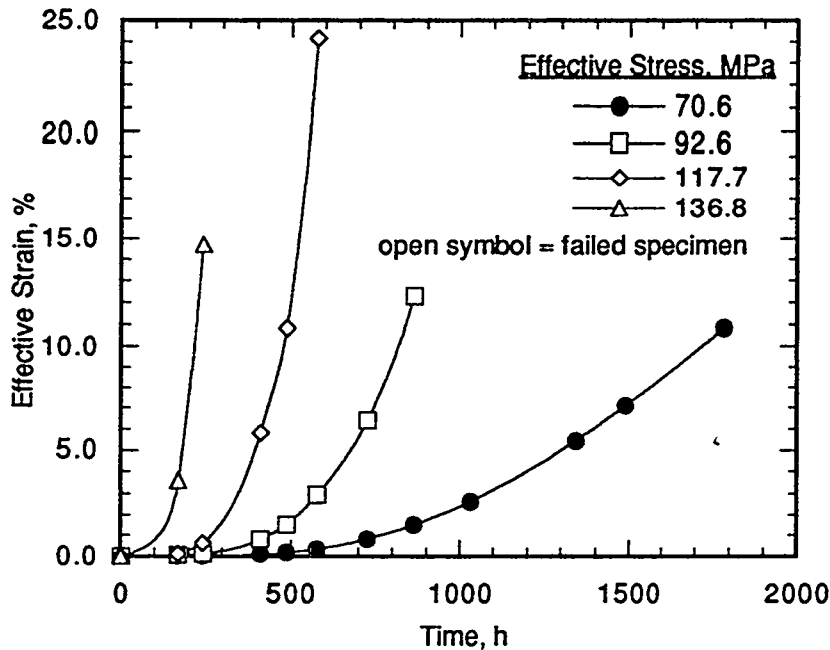


Figure 6. Time dependence of effective mid-wall creep strain at 800°C for unirradiated V-4Cr-4Ti.

### Discussion

It is apparent from the results to date that the creep rate at 800°C is considerably higher than the creep rate at 700°C. For the three highest stresses at 800°C it appears that the secondary creep regime was very short in duration. Even at the lowest stress the results suggest the specimen is exhibiting tertiary rather than secondary creep. Only the highest stress level for the 700°C tests exhibits measurable strain at this juncture. The other stress levels may be too low to cause significant creep at this temperature. These tests will be continued to give an adequate opportunity to accurately measure the secondary creep rate. Significantly more testing is required before meaningful interpretation of the data can be made and comparison of results with those obtained by other investigators.

### FUTURE WORK

Considerable work remains to be done on the specimens which have failed at 800°C. We plan to perform fractographic and microstructural analyses to determine deformation and failure mechanisms. Chemical analyses are also planned to determine if oxygen pickup has influenced the deformation behavior in any way.

## ACKNOWLEDGEMENTS

We acknowledge the substantial contributions of L. K. Fetrow and R. M. Ermi in performing the experiments described in this report.

## REFERENCES

1. K. R. Wheeler, E. R. Gilbert, F. L. Yaggee and S. A. Duran, "Minimum-Creep-Rate Behavior of Polycrystalline Vanadium from 0.35 to 0.87 Tm," *Acta Metallurgica* 19 (1971) 21.
2. M. Shirra, "Das Zeitstandfestigkeits- und Kriechverhalten von Vanadin-Basis-Legierungen," KfK 2440, Kernforschungszentrum Karlsruhe, (1989).
3. H. Boehm and M. Schirra, "Zeitstand und Kriechverhalten von Vanad-Titan und Vanad-Titan-Niob Legierungen," KfK 774, Kernforschungszentrum Karlsruhe, (1968).
4. F. L. Yaggee, Data presented at an AEC/RDT Working Group Meeting, Washington DC (1970).
5. W. Pollack, R. W. Buckman, R. T. Begley, K. C. Thomas and E. C. Bishop, "Development of High Strength Vanadium Alloys - Final Report," WCAP-3487-16, Westinghouse Electric Corporation (1968).
6. T. Kainuma, N. Iwao, T. Suzuki and R. Watanabe, "Creep and Creep Rupture Properties of Unalloyed Vanadium and Solid-Solution-Strengthened Vanadium-Base Alloys," *J. Less Common Metals* 86 (1982) 263.
7. H. M. Chung, B. A. Loomis and D. L. Smith, "Thermal Creep of Vanadium-Base Alloys," in U.S. Contribution, 1994 Summary Report, Task T12: Compatibility and Irradiation Testing of Vanadium Alloys, ANL/FPP/TM-287, ITER/US/95/IV MAT 10 (1995) 87.
8. J. R. Stewart, J. C. LaVake and S. S. Christopher, Data presented at an AEC/RDT Working Group Meeting, Ames, Iowa (1968).
9. A. N. Gubbi, A. F. Rowcliffe, W. S. Eatherly and L. T. Gibson, "Effects of Strain Rate, Test Temperature and Test Environment on Tensile Properties of Vanadium Alloys," in *Fusion Materials: Semiannual Progress Report for Period Ending June 30, 1996*, DOE/ER-0313/20 (1996) 38.
10. S. J. Zinkle, "Thermophysical and Mechanical Properties of V-(4-5)Cr-(4-5)Ti Alloys," in *Fusion Materials: Semiannual Progress Report for Period Ending December 31, 1997*, DOE/ER-0313/23 (1998) 99.
11. M. C. Billone, "Revised ANL-Reported Tensile Data for Unirradiated and Irradiated (FFTF, HFIR) V-Ti and V-Cr-Ti Alloys," in *Fusion Materials: Semiannual Progress Report for Period Ending December 31, 1997*, DOE/ER-0313/23 (1998) 3.

12. M. C. Billone, "Design Lifetime Evaluation for V-4Cr-4Ti First-Wall Structural Material for Fusion Demo Reactors," Argonne National Laboratory, March 25, 1996.
13. H. Tsai, M. C. Billone, R. V. Strain, D. L. Smith and H. Matsui, "Irradiation Creep of Vanadium-Base Alloys," in Fusion Materials: Semiannual Progress Report for Period Ending December 31, 1997, DOE/ER-0313/23 (1998) 149.
14. E. R. Gilbert and L. D. Blackburn, "Creep Deformation of 20 Percent Cold Worked Type 316 Stainless Steel," J. Eng. Mater. & Tech., ASME Trans. (1977) 168.